Golden Jackal Optimization with Neutrosophic Rule-Based Classification System for Enhanced Traffic Sign Detection

Mohammed Assiri[1,*]

[1]Department of Computer Science, College of Computer Engineering and Sciences, Prince Sattam Bin Abdulaziz University, P.O. BOX 16273, Al-Kharj, ZIP 3963, Saudi Arabia.
Emails: m.assiri@psau.edu.sa

Abstract

Traffic signs detection is a critical function of automatic driving and assisted driving is a significant part of Cooperative Intelligent Transport Systems (CITS). The drivers can obtain the data attained via automated traffic sign detection to improve the comfort and security of motor vehicle driving and regulate the behaviors of drivers. Recently, deep learning (DL) has been utilized in the fields of traffic sign detection and achieve better results. But there are two major problems in traffic sign recognition to be immediately resolved. Some false sign is always detected due to the interference caused by bad weather, and illumination variation. Some traffic signs of smaller size are increasingly complex to identify than larger size hence the smaller traffic signs go unnoticed. The objective is to achieve the accuracy and robustness of traffic sign detection for detecting smaller traffic signs in a complex environment. Thus, the study presents a Golden Jackal Optimization with Neutrosophic Rule-Based Classification System (GJO-NRCS) technique for Enhanced Traffic Sign Detection. The GJO-NRCS technique aims to detect the presence of distinct types of traffic signs. In the GJO-NRCS technique, DenseNet201 model is exploited for feature extraction process and the GJO algorithm is used for hyperparameter tuning process. For final recognition of traffic signals, the GJO-NRCS technique applies NRCS technique. The simulation values of the GJO-NRCS method can be examined using benchmark dataset. The experimental results inferred that the GJO-NRCS method reaches high efficiency than other techniques.

Keywords: Traffic Sign Detection; Automatic Driving; Intelligent Transport System; Neutrosophic Rule; Golden Jackal Optimization

1. Introduction

The traffic sign detection system is the data foundation of unmanned driving systems and intelligent transportation systems (ITS), balancing the real-time efficiency and robustness of the traffic sign detection and identification technology that performs a significant role in the decision-making of unmanned driving systems and ITS [1]. Identifying the traffic signs is a vital constituent of intelligent driving system [2]. In real-time applications, traffic sign detection is simply impacted by factors like distance, light intensity, and high-level weather that can improve the security risks related to intelligent vehicles [3]. Traffic sign recognition processes have been generally achieved in natural environments; nevertheless, extreme weather settings (for example, rain, snow, or fog) will unclear traffic signal data, and excessive exposure and blurred light typically decrease the visibility of traffic signs [4]. Moreover, traffic signs have been visible every year, leading to the surface fading, indistinct, or damaged. Intricate and altering surroundings can often impact the precision and speed of traffic sign recognition in ITS. Consequently, it is now particularly important to analyse the issue of accurate and quick traffic sign identification in multifaceted settings [5].

Doi: https://doi.org/10.54216/IJNS.230403
Received: July 26, 2023 Revised: December 02, 2023 Accepted: February 29, 2024

Previous techniques in traffic sign detection employed a sliding window approach to transfer the whole image and produce several candidate fields [6]. The candidate fields have been also extracted with diverse categories of hand-crafted features like HOG, LBP, and SIFT. These features are provided to effective algorithms like RF, Adaboost, and SVM for detection and recognition [7]. However, standard target detection techniques need research workers to manually extract the features and it is strong to modifications. Furthermore, sliding-window-based region selection schemes cannot be directed and extreme time complexity [8]. Recently, majority of object-detection techniques have employed convolutional neural networks (CNNs) and accomplished successful outcomes in target detection tasks like the two-phase detectors region-based Fully connected network (R-FCN), Fast Region CNN (Faster RCNN), YOLO, and one-phase detectors SSD [9]. However, directly implementing such techniques to traffic sign recognition is difficult for achieving reasonable outcomes in real-time applications. The target detection and identification of the vehicle-mounted mobile terminal needs higher necessities for identifying the speed, and higher accuracy for targets of various measures that indicate to fulfil the two desires of real-time and accuracy [10].

This study presents a Golden Jackal Optimization with Neutrosophic Rule-Based Classification System (GJO-NRCS) technique for enhanced Traffic Sign Detection. The GJO-NRCS technique aims to detect the presence of distinct types of traffic signs. In the GJO-NRCS technique, DenseNet201 model is exploited for feature extraction process and the GJO algorithm is used for hyperparameter tuning process. For final recognition of traffic signals, the GJO-NRCS technique applies NRCS technique. The simulation values of the GJO-NRCS method can be examined using benchmark dataset. The experimental results inferred that the GJO-NRCS method reaches high effeceincy than other techniques.

2. Literature Works

Chauhan and Kumar [11] presented an innovative traffic prediction and control technique that is dependent upon wireless sensor networks (WSNs). This is developed by combining the specific features of squawks with the cognitive facets of traffic control and prediction optimization. Primarily, the sensors have been employed followed by the mode-search optimization method proposed. Then, the potential paths could be recognized by employing a multiobjective technique. The developed mode-search-based Deep LSTM (Deep-LSTM) was utilized for prediction and then training with the help of this developed mode-search optimization. In [12], a new classification method was introduced. The research workers primarily employed Kernel PCA (KPCA) technique for minimizing the features of the chosen databases. To improve classification method, an optimum rule was produced in Neutrosophic Set (NS) as well as its rule optimization, Oppositional-based Elephant Herd Algorithm (OEHA) could be exploited. Then, choosing the features, Deep Learning (DL) technique has been presented for categorizing the data. Mirza and Samak [13] projected a unique technique for precisely categorizing chest X-ray (CXR) images in COVID19 forecast by integrating Neutrosophic Fuzzy Logic (FL) with the Hybrid LSTM and CNN model. The proposed hybrid technique employs the benefits of LSTM for sequential data learning and CNN for feature extraction. Hybrid CNN-LSTM model was dependent upon Neutrosophic FL was trained under massive sets of diverse CXR images. The fusion of Neutrosophic FL with a Hybrid CNN-LSTM model makes a robust architecture for handling classification tasks.

Keerthi and Santhi [14] Considered majorly in medical image processing. Firstly, the median filter (MF) was essentially implemented for removal of noise reduction. The graph-cut segmentation algorithm has been exploited for segmentation. The removed feature must be chosen by employing the Ant Colony Optimization (ACO) technique. The Euclidean distance can be applied to computing the range of similarity. The chosen feature values are specified to the Relevance Vector Machine (RVM) which has a multiclass classification method. In conclusion, the cancer has been categorized into CNN for feature extraction normal and abnormal. Essameldin et al. [15] implemented a neutrosophic-based OM technique. A social network analysis (SNA) should be performed through prevalent SNA tools (for example, Graphistry) for interpretations. An effect weighting of clients should be executed employing an artificial neural network (ANN) that is dependent upon the SNA offered output and responses of individuals to the OM examined texts. The OM scores required for combination were produced employing the TextBlob.

In [16], an interval type-2 (IT2) mutual subsethood Cauchy fuzzy neural inference model (T2MSCFuNIS) was developed in this study. A volume defuzzification was utilized for calculating the numerical output. A gradient descent backpropagation (GDP) model is employed for training. Primarily, the Cauchy-MF (CMF) was utilized as alternative potent fuzzy basis function (FBF) system. Secondarily, computation of the mutual subsethood similarity estimation among the IT2CMFs as well as upgrading formulae of every model parameter in analytic closed-form equations. Lastly, the capability to remove the type-1 (T1-MSCFuNIS) with each analytic closed-form equation. Darwish et al. [17] presented a technique for identifying internal objects by employing a neutrosophic logic (NL) and rotational ultrasonic array. An NS was the subsequent development of the fuzzy set owing to its indefinite membership values

Doi: https://doi.org/10.54216/IJNS.230403
Received: July 26, 2023 Revised: December 02, 2023 Accepted: February 29, 2024

that will be inattentive from traditional fuzzy sets. The developed technique could be made to consider the wall location and also control the VIP for easily moving (for example, right, ahead, and left) reliant on the level of reliability.

3. The Proposed Method

In this study, we have presented a GJO-NRCS method for enhanced traffic sign detection. The GJO-NRCS technique aims to detect the presence of distinct types of traffic signs. It contains different subprocesses such as DenseNet201-based feature extraction, GJO-based hyperparameter tuning, and NRCS for traffic sign detection. Fig. 1 depicts the entire procedure of the GJO-NRCS technique.

A. DenseNet201 Model

Initially, the GJO-NRCS method, and DenseNet201 model is exploited to feature extraction process. In comparison with classical ML approaches, CNN can automatically learn and characterize complex features that rely on handcrafted features [18]. Meanwhile, CNN-based model differs with respect to fully connected layer, convolutional (Conv) layer, size of kernel, and pooling operation. The feature is extracted from the pretrained CNN models such as EfficientNet, VGG, SqueezeNet, Inception, DenseNet, and ResNet. Generally, deep convolutional neural network is (DCNN) the most efficient image recognition framework due to its unique sort of pooling and convolutional layers. DCNN architecture focuses on making the DL network go deep, however simultaneously making it better to train, through shortcut connections between these layers. However, the gradient or input data flow through most of the levels dissipates as the network becomes deep. DenseNet solves the gradient disappearing problems by connecting each layer with equivalent feature sizes with one another. As the ideal model, this study presents DenseNet201 for the feature extraction stage.

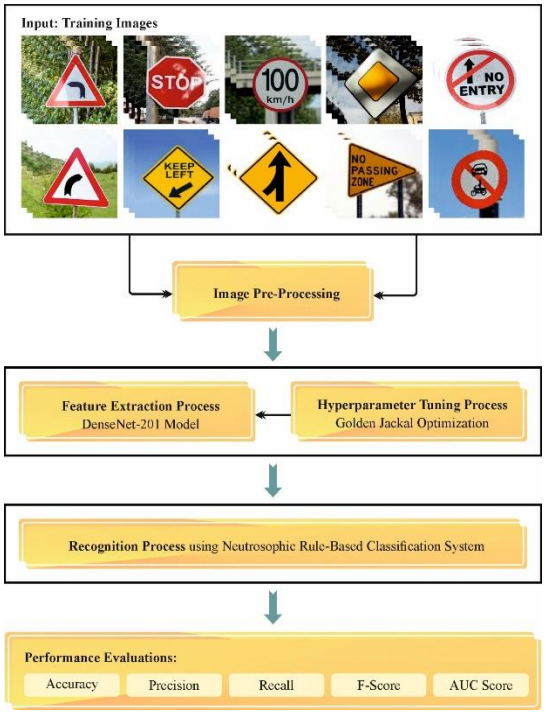

Figure 1: Overall process of GJO-NRCS technique

DenseNet201 is a CNN with 201 layers. It is used to load a pretrained model that is trained on over a billion images through the ImageNet dataset. The model classifies images into 1000 groups of objects. Subsequently, the model has learned a feature representation for different types of images. The dimension of input image is 224×224. Deep the network, the more collective features can be gathered. The major concern is the capability to concatenate the generated feature map by all the layers for providing the input for the succeeding layer. This shows that there are links between all other layers and resolves the gradient vanishing problems.

Doi: https://doi.org/10.54216/IJNS.230403
Received: July 26, 2023 Revised: December 02, 2023 Accepted: February 29, 2024

The DenseNet201 model has approximately 20 million parameters and 708 layers. The architecture contains input layer, the image size 224 × 224, 4 dense blocks performed by 1×1 Conv layer before the 3×3 Conv layers, minimize the computation cost and feature map; there are 3 transition layers namely 1×1 Conv layer, and batch normalization layer; average pooling layer is same as classical pooling approach except it decreases the feature map, having the dropout layer with 0.2 dropout rate, and avoid over-fitting; the last layer is Softmax and FC layer. Non-linear transformations like batch normalization (BN), ReLu, pooling, and convolution (Conv), are performed in all the layers of DenseNet201. The DenseNet201 architecture makes use of the weight it has learned from the ImageNet database to diminish computational workload and the transfer learning is used for the automatic feature extraction, allowing the conception of uncomplicated and simple models, and feature is reused over layers, permitting for higher performance and more diversity and boosting the efficiency of the model parameter. The architecture uses a feedforward approach for connecting all the layers. The infrastructure of DenseNet201 is illustrated in Fig. 2.

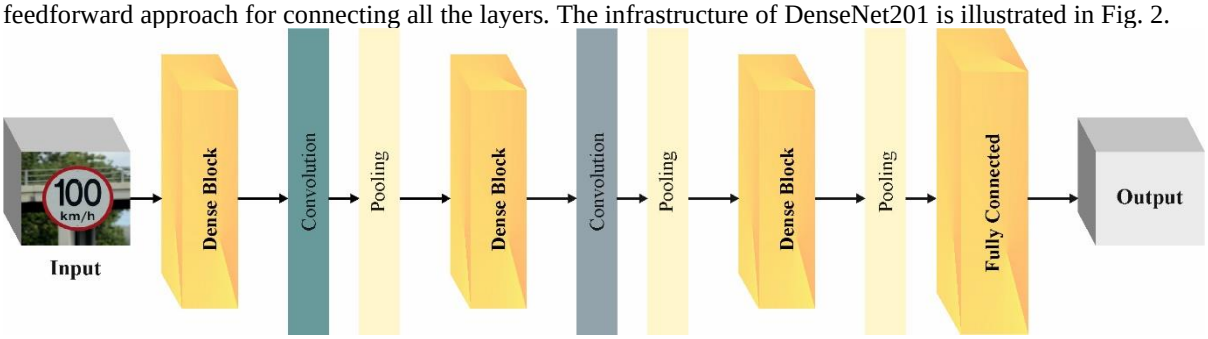

Figure 2: Framework of DenseNet201

B. Hyperparameter Tuning using GJO

In this phase, the GJO technique is utilized for the hyperparameter tuning process. The GJO is a new SI optimization that mimics the natural hunting strategy of golden jackals (GJ) [19]. Their group hunting has female and male individuals. It comprises 3 stages in their hunting strategy such as searching for and approaching prey, neighbouring and confusing the prey, swooping on the prey, and terminating its effort.

During the initial stage, the group of prey positions matrix (Prey (0)) can be arbitrarily made by Eq. (1).

$$Prey(0) = \begin{bmatrix} L_{11} & L_{1,2} & \cdots & L_{1,dim} \\ L_{21} & L_{2,2} & & L_{2,dim} \\ & \vdots & \ddots & \vdots \\ L_{pop,1} & L_{pop,2} & \cdots & L_{pop,dim} \end{bmatrix} \quad (1)$$

whereas pop defines the prey population and dim stands for the dimension.

E refers to the evading energy of the prey and is evaluated employing Eq. (1).

$$E = E_1 \cdot E_0 \quad (2)$$

In which, E_1 and E_0 signifies the reducing prey energy and preliminary energy, correspondingly. Value of E_0 from the interval of one and one, but the value of E_1 is measured employing Eq. (3).

$$E_1 = c_1 \cdot \left(1 - \frac{ite}{\max\_ite}\right) \quad (3)$$

Whereas c_1 is set to 1.5, ite illustrates the present iteration, and $\max\_ite$ implies the higher iteration counter.

When $|E| > 1$, GJ pursuing is mathematically expressed utilizing in Eqs. (4) and (5):

$$L_1(ite) = L_M(ite) - E \cdot |L_M(ite) - rlPrey(ite)| \quad (4)$$

$$L_2(ite) = L_{FM}(ite) - E \cdot |L_{FM}(ite) - rlPrey(ite)| \quad (5)$$

whereas $L_1(ite)$ and $L_2(ite)$ represents the upgrade locations male GJ and female GJ, correspondingly, $L_M(ite)$ and $L_{FM}(ite)$ defines the position of male GJ and female GJ, rl denotes the random vector number evaluated employing Levy's flight (LF) strategy, $Prey(ite)$ signifies the vector of prey positions, $|L_M(ite) - rl \cdot Prey(ite)|$ implies the spacing among the prey and GJ, and rl refers to the arbitrary vector evaluated utilizing the LF strategy as specified in Eqs. (6) & (7).

$$rl = 0.05 \cdot Lf(z) \quad (6)$$

Doi: https://doi.org/10.54216/IJNS.230403
Received: July 26, 2023 Revised: December 02, 2023 Accepted: February 29, 2024

$$Lf(z) = \frac{0.01 \cdot u \cdot \sigma}{\left| v^{\left(\frac{1}{\beta}\right)} \right|}; \sigma = \left[\frac{\Gamma(1+\beta) \cdot \sin\frac{\pi \cdot \beta}{2}}{\Gamma\left(\frac{1+\beta}{2}\right) \cdot \beta \cdot (2\beta - 1)} \right]^{1/\beta} \quad (7)$$

whereas u and v are arbitrarily well-defined values among 0 and 1; β is set to 1.5.
Although the prey can be exhausted owing to the chasing, E is reduced, once $|E| \leq 1$, the jackals neighboring the prey and consume it utilizing Eqs. (8) and (9):

$$L_1(ite) = L_M(ite) - E \cdot |rl \cdot L_M(ite) - Prey(ite)| \quad (8)$$

$$L_2(ite) = L_{FM}(ite) - E \cdot |rl \cdot L_{FM}(ite) - Prey(ite)| \quad (9)$$

The upgraded prey position $\left(L(ite+1)\right)$ is evaluated by deploying the average of $L_1(ite)$ and $L_2(ite)$ as written in Eq. (10).

$$L(ite+l) = \frac{(L_1)(ite) + L_2(ite)}{2} \quad (10)$$

The GJO method derives an FF to achieve high classifier outcomes. It defines a positive integer to represent the superior performance of the solution candidate. Here, the minimization of the classifier error rate is considered as the FF.

$$fitness(x_i) = ClassifierErrorRate(x_i) = \frac{number\ of\ misclassified\ samples}{Total\ number\ of\ samples} * 100 \quad (11)$$

C. NRCS for Traffic Sign Detection

The GJO-NRCS technique applies NRCS technique for final recognition of traffic signals. Neutrosophic was developed to switch imperfect and uneven data without risk of trivialization [20]. Neutrosophy is a novel division of philosophy, with early origins, managing neutralities and their contacts with dissimilar ideas.
This theory studies each concept $< X >$ organized with the neutralities range <NeutX > which is either $< X >$ or <AntiX > and reverse or negative <AntiX>. The <NeutX > and <AntiX > can measured as $< Non\ X >$. As per the theory, $< X >$ inclines to be stable and defused by <Anti $X >$ and $< Non\ X >$.
Neutrosophic logic was presented in order to signify accurate method of incompleteness, contradiction, vagueness, imprecision, uncertainty, redundancy, inconsistency and ambiguity.
Neutrosophic logic is a reason in which every plan has been assessed to consume the ratio of reality in the subset T, the indeterminacy ratio in the subset I, and the falsity ratio in the subset F, whereas T, I, and F are non-standard and standard actual subset of $]^{-}0, 1^{+}[$.
with

$$\sup T = t\_\sup, infT = t\_\inf \quad (12)$$

$$\sup I = i\_sup\ , infI = i\_inf \quad (13)$$

$$sup\ F = f\_sup, infF = f\_inf \quad (14)$$

and

$$n\_\sup = t\_\sup\ + i\_\sup\ + f\_\sup \quad (15)$$

$$n\_\inf = t\_\inf\ + i\_\inf\ + f\_\inf. \quad (16)$$

Where F, T, and I are known as neutrosophic components signifying the falsehood, truth and indeterminacy values, correspondingly.
In real uses, it is very simple to utilize normal actual range of [0 and1] for T, I, and F in its place of non-standard unit range $]^{-}0, 1^{+}[$. In neutrosophic logic, all factors are vital to human thought. Occasionally, we are inclined to complete/justice in certain situations. Inaccuracy of human methods owing to the deficiency of data obtains from the exterior world. The vital notions of neutrosophic set deliver a natural basis for handling the neutrosophic phenomena which exist widely and for constructing novel divisions of neutrosophic arithmetic.
Now we describe a formal explanation. Let's assume X be an object space, with a general component x in X. The neutrosophic set A in X is considered by I_A, F_A and T_A membership functions which signifies an indeterminacy, a falsity, and a truth respectively. Whereas $T_A(x)$, $I_A(x)$ and $F_A(x)$ indicates the real non-standard or standard subset of range $]^{-}0, 1^{+}[$.

$$T_A: X \rightarrow]^{-}0, 1^{+}[\quad (17)$$

$$I_A: X \rightarrow]^{-}0, 1^{+}[\quad (18)$$

$$F_A: X \rightarrow]^{-}0, 1^{+}[\quad (19)$$

Doi: https://doi.org/10.54216/IJNS.230403
Received: July 26, 2023 Revised: December 02, 2023 Accepted: February 29, 2024

It has no constraint on the summation of higher $I_A(x)$ $I_A(x)$ and (x), thus $-0 \leq supT_A(x) + supI_A(x) + supF_A(x) \leq 3^3$.

The NRCS makes use of NL for the generalization of fuzzy rule-based classification system [21]. Rather than fuzzy logic, the consequents and antecedents of the "IF-THEN" rules are NL statements in the NRCS. The three different phases of NRCS are

- Neutrosophication: The neutrosophic crisp input is converted into truth, falsity, and indeterminacy memberships.
- Inference engine: The KB and neutrosophic "IF-THEN" rule is used to obtain a neutrosophic output.
- Deneutrosophication: The neutrosophic output of prior step is converted into crisp values using the above three membership functions.

The KB stores the available knowledge as neutrosophic "IF − THEN" rules, and later using the neutrosophic set, they capture neutrosophic rule semantics. Data extraction, neutrosophication, rules generation, and classification are the four different stages of NRCS. In the following sections, each phase of NRCS is given.

1. Data extraction stage

Here, data is extracted through the data files and extracting (1) the maximum and minimum values of the feature, (2), number of attributes, (3) class labels or decisions, and (4) number of classes and their names.

Neutrosophication stage

The above three membership functions are defined in this stage. The membership function is extracted from fuzzy-trapezoidal membership function. The neutrosophic component $\langle T, I, F \rangle$ represent all the attribute values in neutrosophic form. The above three membership functions are exploited on feature value of the dataset to get the three elements.

2. Rules generation phase

The objective is to construct rules. Consider $X = \{x_1, x_2, \dots, x_n\}$, in which x_i denotes the i^{th} samples and n indicates the overall amount of samples. Every sample has single class label as $c_i \in \{1,2, \dots, C\}$, in which C specifies the overall amount of classes. Firstly, the data is divided into testing data ($X_{testing}$) without class labels and training data ($X_{training}$) with class label. The accurate neutrosophic rule is generated from the testing and training dataset. In NRCS, all the attributes in neutrosophic rule contain three elements that define the degree of truth, degree of indeterminacy, and degree of falsity.

3. Classification phase

The testing rules without class labels is generated. If ($x_t \in X_{testing}$), then the intersection ratio is evaluated between the testing and training rules ($X_{training}$), and the percentage was represented as $P = \{p_1, p_2, \dots, p_q\}$, where the matching ratio between x_t and x_i is denoted as $p_i$and the number of rules in the training set is q. The class labels of training rules with maximal percentages are allocated to the testing rules. There is no connection between the training and testing rules if ($p_i < 0.5, \forall i = 1, \dots, q$), then class labels are derived from the exact rule set. Next, add testing rules to the training rule rather than testing rule ($X_{training} = X_{training} \cup x_t$).

Lastly, compared with the exact matrix, the testing matrix has prediction class label has original class label. The confusion matrix is computed to evaluate our model. The true negative (TN), false negative (FN), true positive (TP), and false positive (FP) are different measures that can be calculated from the confusion matrix.

4. Result Analysis

The performance analysis of the GJO-NRCS system takes place under the traffic sign dataset, which contains 1500 samples and 10 classes as represented in Table 1.

Table 1: Details of database

Classes	Labels	No. of Samples
Speed limit(100 km/h)	C-1	150
No passing	C-2	150
Priority road	C-3	150
Stop	C-4	150
No vehicles	C-5	150
No entry	C-6	150

Doi: https://doi.org/10.54216/IJNS.230403
Received: July 26, 2023 Revised: December 02, 2023 Accepted: February 29, 2024

Dengerous curve to the left	C-7	150
Dangerous curve to the right	C-8	150
Keep right	C-9	150
Keep left	C-10	150
Total No. of Samples		1500

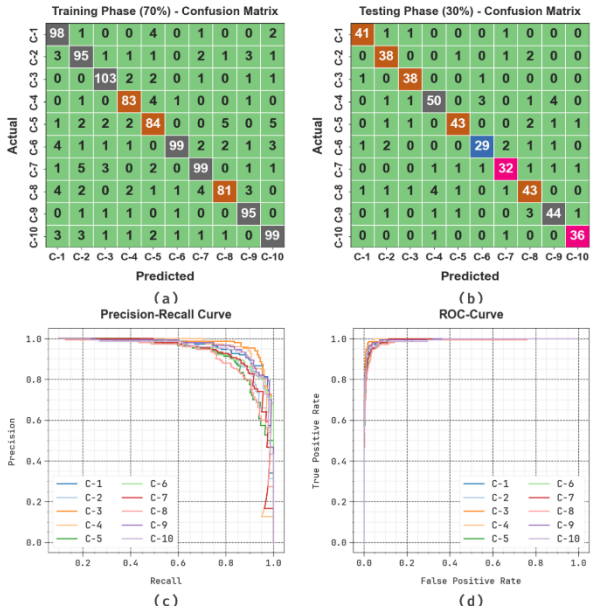

Figure 3: Classifier outcome of (a-b) Confusion matrices and (c-d) PR and ROC curves

The classifier outcomes of the GJO-NRCS method on test dataset is demonstrated in Fig. 3. The confusion matrices offered by the GJO-NRCS system under 70:30 of TRAPH/TESPH is depicted in Figs. 3a-3b. The figure signified that the GJO-NRCS algorithm has accurately detected and classified all 10 classes. Likewise, the PR analysis of the GJO-NRCS technique is demonstrated on Fig. 3c. The figure indicated that the GJO-NRCS technique has gained maximum PR performance under all classes. Lastly, the ROC study of the GJO-NRCS technique is illustrated in Fig. 3d. The figure portrayed that the GJO-NRCS method has resulted in promising outcomes with maximum ROC values on distinct class labels.

The recognition outcomes of the GJO-NRCS system are provided in Table 2 and Fig. 4. The outcomes imply that the GJO-NRCS method properly recognizes distinct classes of traffic signals. With 70%TRAPH, the GJO-NRCS algorithm provides average $accu_y$ of 97.83%, $prec_n$ of 89.17%, $reca_l$ of 89.17%, F_{score} of 89.11%, and AUC_{score} of 93.98%. Also, with 30%TESPH, the GJO-NRCS technique offers average $accu_y$ of 97.51%, $prec_n$ of 87.65%, $reca_l$ of 87.82%, F_{score} of 87.70%, and AUC_{score} of 93.22%.

Table 2: Recognition results of the GJO-NRCS technique under 70:30 of TRAPH/TESPH

Class Labels	$Accu_y$	$Prec_n$	$Reca_l$	F_{Score}	AUC_{Score}
TRAPH (70%)					
C-1	97.71	85.96	92.45	89.09	95.38
C-2	97.24	85.59	87.96	86.76	93.13
C-3	98.48	91.96	93.64	92.79	96.34
C-4	98.38	89.25	92.22	90.71	95.59

Doi: https://doi.org/10.54216/IJNS.230403
Received: July 26, 2023 Revised: December 02, 2023 Accepted: February 29, 2024

C-5	96.86	84.00	83.17	83.58	90.74
C-6	98.19	96.12	86.84	91.24	93.21
C-7	97.71	90.00	88.39	89.19	93.61
C-8	97.52	90.00	82.65	86.17	90.85
C-9	98.67	90.48	95.96	93.14	97.45
C-10	97.52	88.39	88.39	88.39	93.50
Average	97.83	89.17	89.17	89.11	93.98
TESPH (30%)					
C-1	98.67	93.18	93.18	93.18	96.22
C-2	97.56	84.44	90.48	87.36	94.38
C-3	98.67	90.48	95.00	92.68	97.01
C-4	96.22	87.72	83.33	85.47	90.77
C-5	97.78	91.49	87.76	89.58	93.38
C-6	97.33	85.29	80.56	82.86	89.67
C-7	97.33	84.21	84.21	84.21	91.38
C-8	95.78	81.13	82.69	81.90	90.09
C-9	96.89	86.27	86.27	86.27	92.26
C-10	98.89	92.31	94.74	93.51	97.00
Average	97.51	87.65	87.82	87.70	93.22

The performance of the GJO-NRCS technique is graphically represented in Fig. 5 in the form of training accuracy (TRAA) and validation accuracy (VALA) curves. The figure shows useful interpretation of the behavior of the GJO-NRCS method over various epoch counts, demonstrating its learning process and generalization abilities. Remarkably, the figure indicates the steady improved in the TRAA and VALA with progress in epochs. It ensures the adaptive nature of the GJO-NRCS method in the pattern recognition process on TRA and TES dataset. The rising trend in VALA outlines the ability of GJO-NRCS technique to adapt to the TRA data and also excels in providing accurate classification of hidden data, pointing out strong generalizability.

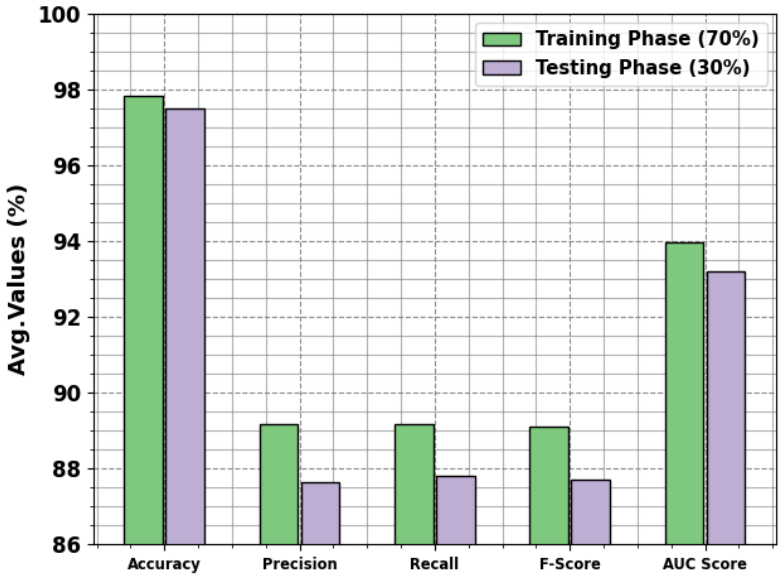

Figure 4: Average of GJO-NRCS technique under 70:30 of TRAPH/TESPH

Doi: https://doi.org/10.54216/IJNS.230403
Received: July 26, 2023 Revised: December 02, 2023 Accepted: February 29, 2024

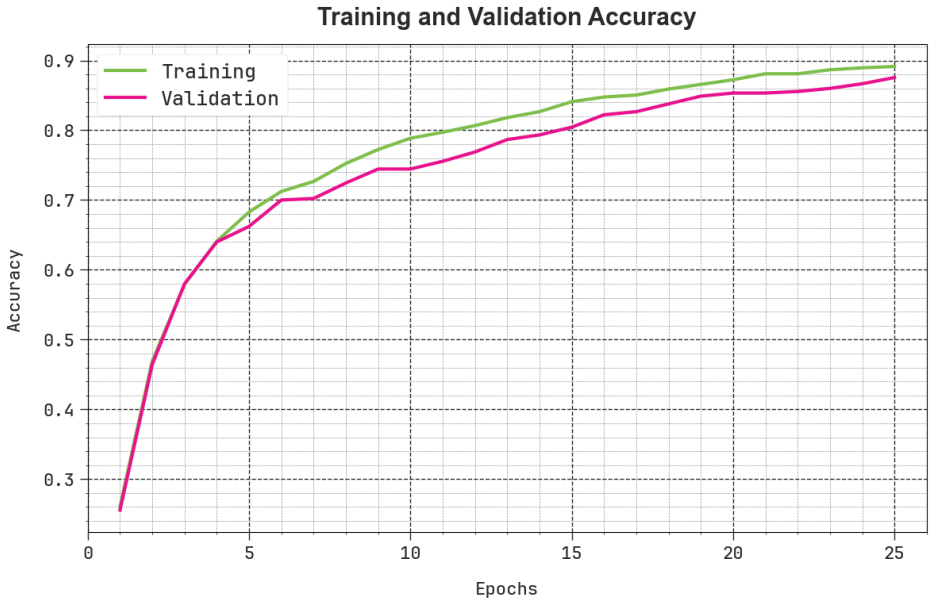

Figure 5: $Accu_y$ curve of the GJO-NRCS method

A complete representation of the training loss (TRLA) and validation loss (VALL) outcomes of the GJO-NRCS model over distinct epochs is demonstraed in Fig. 6. The progressive decline in TRLA highlights the GJO-NRCS model optimizing the weights and reducing the classifier error on the TRA and TES dataset. The figure shows a clean understanding of the GJO-NRCS model's association with the TRA data, highlighting its proficiency in capturing pattern within both datasets. Remarkably, the GJO-NRCS method continually enhances its parameters in decreasing the differences between the prediction and real TRA class labels.

Figure 6: Loss curve of the GJO-NRCS technique

Table 3 represents a brief comparison study of the GJO-NRCS technique [22]. The comparative outcome of the GJO-NRCS method in terms of $accu_y$ is demonstrated in Fig. 7. Based on $accu_y$, the GJO-NRCS technique offers higher $accu_y$ of 97.83% while the HOG-RF, Gabor+LBP+HOG, HOG-SVM, CLBP-SVM, HOG+CLBP, HOG+Gabor, and CLBP+Gabor models have shown lower $accu_y$ of 97.20%, 97.04%, 95.70%, 96.88%, 97.03%, 96.90%, and 96.40%, correspondingly. Fig. 8 demonstrates the comparative outcomes of the GJO-NRCS method in terms of $prec_n$, $reca_l$,

Doi: https://doi.org/10.54216/IJNS.230403
Received: July 26, 2023 Revised: December 02, 2023 Accepted: February 29, 2024

and F_{score}. Based on $prec_n$, the GJO-NRCS technique offers higher $prec_n$ of 89.17% while the HOG-RF, Gabor+LBP+HOG, HOG-SVM, CLBP-SVM, HOG+CLBP, HOG+Gabor, and CLBP+Gabor techniques have shown lower $prec_n$ of 84.35%, 74.92%, 85.11%, 78.77%, 81.95%, 87.18%, and 80.65%, correspondingly.

Table 3: Comparative analysis of GJO-NRCS method with existing techniques

Classifiers	$Accu_y$	$Prec_n$	$Reca_l$	F_{score}
GJO-NRCS	97.83	89.17	89.17	89.11
HOG-Random Forest	97.20	84.35	82.69	77.67
Gabor+LBP+HOG	97.04	74.92	79.06	78.98
HOG-SVM	95.70	85.11	84.02	84.42
CLBP-SVM	96.88	78.77	81.09	75.35
HOG+CLBP	97.03	81.95	86.25	86.17
HOG+Gabor	96.90	87.18	81.32	83.26
CLBP+Gabor	96.40	80.65	75.76	78.14

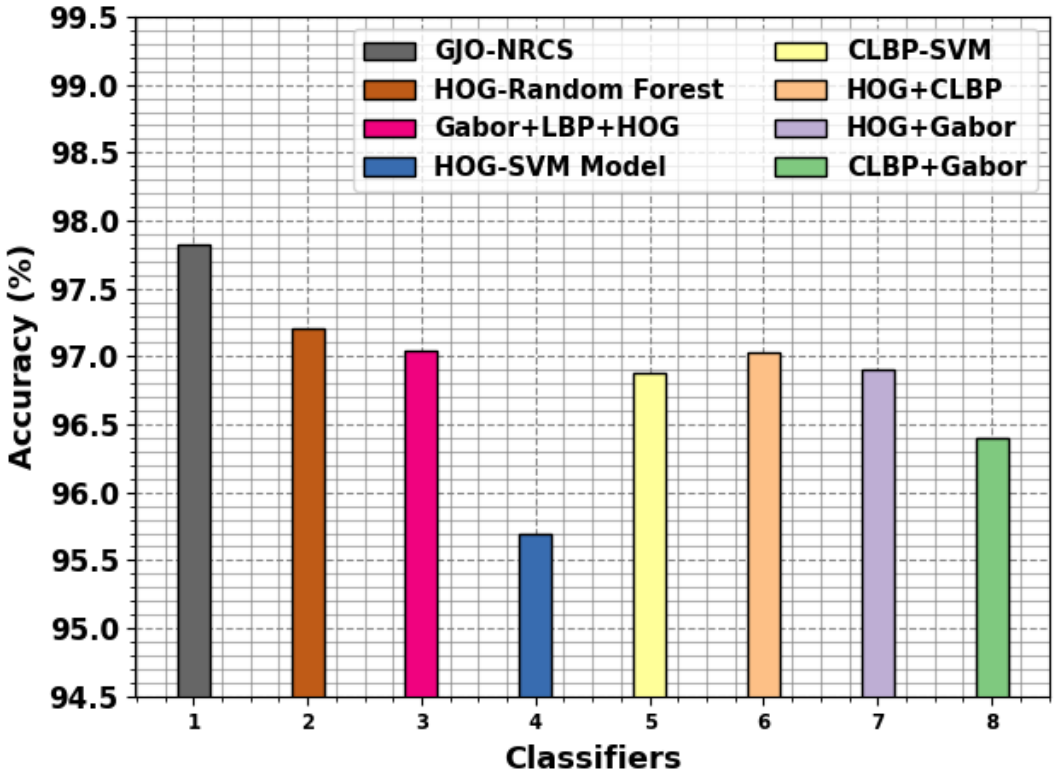

Figure 7: $Accu_y$ analysis of GJO-NRCS method with existing techniques

Doi: https://doi.org/10.54216/IJNS.230403
Received: July 26, 2023 Revised: December 02, 2023 Accepted: February 29, 2024

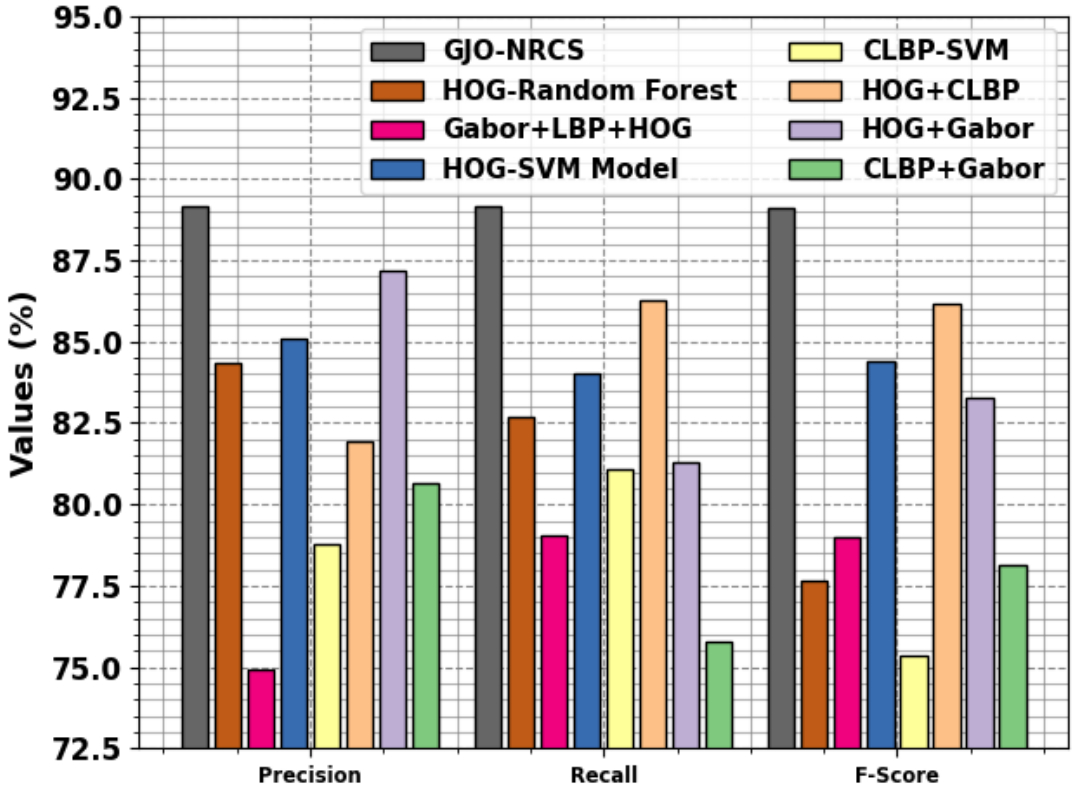

Figure 8: Comparative analysis of GJO-NRCS method with existing techniques

Moreover, based on $reca_l$, the GJO-NRCS technique offers higher $reca_l$ of 89.17% while the HOG-RF, Gabor+LBP+HOG, HOG-SVM, CLBP-SVM, HOG+CLBP, HOG+Gabor, and CLBP+Gabor approaches have shown lower $reca_l$ of 82.69%, 79.06%, 84.02%, 81.09%, 86.25%, 81.32%, and 75.76%, correspondingly. Lastly, based on F_{score} the GJO-NRCS method offers higher F_{score} of 89.11% while the HOG-RF, Gabor+LBP+HOG, HOG-SVM, CLBP-SVM, HOG+CLBP, HOG+Gabor, and CLBP+Gabor method have illustrated lower F_{score} of 77.67%, 78.98%, 84.42%, 75.35%, 86.17%, 83.26%, and 78.14%, correspondingly. Thus, the GJO-NRCS technique can be used for effectual traffic sign recognition process.

5. Conclusion

In this study, we have presented a GJO-NRCS method for enhanced traffic sign detection. The GJO-NRCS technique aims to detect the presence of distinct types of traffic signs. It contains different subprocesses such as DenseNet201-based feature extraction, GJO-based hyperparameter tuning, and NRCS for traffic sign detection. At the primary level, the GJO-NRCS technique, DenseNet201 model is exploited for feature extraction process and the GJO algorithm is used for hyperparameter tuning process. For final recognition of traffic signals, the GJO-NRCS technique applies NRCS technique. The simulation results of the GJO-NRCS method can be examined using benchmark dataset. The experimental outcomes inferred that the GJO-NRCS method reaches higher efficiency than other techniques"

Funding: "This research received no external funding"

Conflicts of Interest: "The authors declare no conflict of interest."

Acknowledgment : "The author extends his appreciation to Prince Sattam bin Abdulaziz University for funding this research work through the project (PSAU/2023/01/25212).

References

[1] Kaplan Berkaya, S.; Gunduz, H.; Ozsen, O.; Akinlar, C.; Gunal, S. On Circular Traffic Sign Detection and Recognition. Expert Syst. Appl. 2016, 48, 67–75.

Doi: https://doi.org/10.54216/IJNS.230403
Received: July 26, 2023 Revised: December 02, 2023 Accepted: February 29, 2024

[2] He, X.; Dai, B. A New Traffic Signs Classification Approach Based on Local and Global Features Extraction. In Proceedings of the 2016 6th International Conference on Information Communication and Management (ICICM), Hatfield, UK, 29–31 October 2016; pp. 121–125.
[3] X. Xu, J. Jin, S. Zhang, L. Zhang, S. Pu, and Z. Chen, ''Smart data driven traffic sign detection method based on adaptive color threshold and shape symmetry,'' Future Gener. Comput. Syst., vol. 94, pp. 381–391, May 2019.
[4] Y. Yang and F. Wu, ''Real-time traffic sign detection via color probability model and integral channel features,'' in Proc. Chin. Conf. Pattern Recognit. (CCPR), CCIS, vol. 484, 2014, pp. 545–554.
[5] Rajendran, S.P.; Shine, L.; Pradeep, R.; Vijayaraghavan, S. Real-Time Traffic Sign Recognition Using YOLOv3 Based Detector. In Proceedings of the 2019 10th International Conference on Computing, Communication and Networking Technologies (ICCCNT), Kanpur, India, 6–8 July 2019; pp. 1–7.
[6] H. S. Lee and K. Kim, ''Simultaneous traffic sign detection and boundary estimation using convolutional neural network,'' IEEE Trans. Intell. Transp. Syst., vol. 19, no. 5, pp. 1652–1663, May 2018.
[7] T. Yang, X. Long, A. K. Sangaiah, Z. Zheng, and C. Tong, ''Deep detection network for real-life traffic sign in vehicular networks,'' Comput. Netw., vol. 136, pp. 95–104, May 2018.
[8] Y. Yuan, Z. Xiong, and Q. Wang, ''VSSA-NET: Vertical spatial sequence attention network for traffic sign detection,'' IEEE Trans. Image Process., vol. 28, no. 7, pp. 3423–3434, Jul. 2019.
[9] L. Yu, X. Xia, and K. Zhou, ''Traffic sign detection based on visual cosaliency in complex scenes,'' Appl. Intell., vol. 49, no. 2, pp. 764–790, Feb. 2019.
[10] H. Luo, Y. Yang, B. Tong, F. Wu, and B. Fan, ''Traffic sign recognition using a multi-task convolutional neural network,'' IEEE Trans. Intell. Transp. Syst., vol. 19, no. 4, pp. 1100–1111, Apr. 2018.
[11] Gomathy, V., Jayasankar, T., Rajaram, M., Devi, E.A. and Priyadharshini, S., 2022. Optimal neutrosophic rules based feature extraction for data classification using deep learning model. In Soft Computing for Data Analytics, Classification Model, and Control (pp. 57-79). Cham: Springer International Publishing.
[12] Mirza, O.M. and Samak, A.H., 2024. Neutrosophic Fuzzy Logic-Based Hybrid CNN-LSTM for Accurate Chest X-ray Classification in COVID-19 Prediction. Sciences, 18(1), p.14.
[13] Keerthi, S. and Santhi, P., 2023. Precise multi-class classification of brain tumor via optimization based relevance vector machine. Intelligent Automation and Soft Computing, 36(1), pp.1173-1188.
[14] Essameldin, R., Ismail, A.A. and Darwish, S.M., 2022. Quantifying Opinion Strength: A Neutrosophic Inference System for Smart Sentiment Analysis of Social Media Network. Applied Sciences, 12(15), p.7697.
[15] Hefny, H.A. and Amer, N.S., 2024. Interval Type-2 Mutual Subsethood Cauchy Fuzzy Neural Inference System (IT2MSCFuNIS). International Journal of Computational Intelligence Systems, 17(1), pp.1-23.
[16] Darwish, S.M., Salah, M.A. and Elzoghabi, A.A., 2023. Identifying Indoor Objects Using Neutrosophic Reasoning for Mobility Assisting Visually Impaired People. Applied Sciences, 13(4), p.2150.
[17] Chauhan, S.S. and Kumar, D., 2023. Mode Search Optimization Algorithm for Traffic Prediction and Signal Controlling Using Bellman–Ford with TPFN Path Discovery Model Based on Deep LSTM Classifier. SN Computer Science, 4(5), p.686.
[18] Rashed, B.M. and Popescu, N., 2024. Medical Image-Based Diagnosis Using a Hybrid Adaptive Neuro-Fuzzy Inferences System (ANFIS) Optimized by GA with a Deep Network Model for Features Extraction. Mathematics, 12(5), p.633
[19] Agwa, A.M., Alanazi, T.I., Kraiem, H., Touti, E., Alanazi, A. and Alanazi, D.K., 2023. MPPT of PEM Fuel Cell Using PI-PD Controller Based on Golden Jackal Optimization Algorithm. Biomimetics, 8(5), p.426.
[20] Basha, S.H., Abdalla, A.S. and Hassanien, A.E., 2016, December. Gnrcs: hybrid classification system based on neutrosophic logic and genetic algorithm. In 2016 12th International Computer Engineering Conference (ICENCO) (pp. 53-58). IEEE.
[21] Basha, S.H., Abdalla, A. and Hassanien, A.E., 2021. Neutrosophic rule-based classification system and its medical applications. In Big Data in Psychiatry# x0026; Neurology (pp. 119-135). Academic Press.
[22] Triki, N., Karray, M. and Ksantini, M., 2023. A real-time traffic sign recognition method using a new attention-based deep convolutional neural network for smart vehicles. Applied Sciences, 13(8), p.4793.

Doi: https://doi.org/10.54216/IJNS.230403
Received: July 26, 2023 Revised: December 02, 2023 Accepted: February 29, 2024